



A new methodology exploring the record of snow avalanches in lake sediments

Laurent Fouinat¹, Pierre Sabatier¹, Jérôme Poulenard¹, Jean-Louis Reyss², Xavier Montet³, Fabien Arnaud¹.

5

¹EDYTEM, Université Savoie Mont Blanc, CNRS 73376 Le Bourget du Lac Cedex, France

²LSCE, Université de Versailles Saint-Quentin CEA-CNRS, avenue de la Terrasse, 91198 Gif-sur-Yvette cedex, France

10 ³University of Geneva Department of Radiology and Medical Informatics Genève, Rue Gabrielle-Perret-Gentil 4, CH-1211, Switzerland

15

Correspondence to: Laurent Fouinat (laurent.fouinat@univ-smb.fr)

20

25

30

35

40

45

50



Abstract. In recent years, wet avalanche deposits have become a subject of increasing concern in a context of both global change and winter mountain tourism activities. This study focuses on the use of a new methodology based on CT scans to identify snow avalanche deposits in lake sediment. Here, we study the mid-elevation Lake Lauvitel system (western French Alps), which features steep slopes and avalanche corridors. CT scanning is a fast, non-destructive method based on X-ray technology and allows the identification of elements with different densities. We applied this method to sediment cores, leading to the 3D identification of the dense rocks and organic matter macroremains that characterize wet avalanches. A total of eight periods of higher avalanche activity are identified since AD 1880 at the site. This new methodology is suitable for avalanche deposit reconstruction and may be applicable more widely in paleolimnological studies.

1 Introduction

Snow avalanches are a natural hazard presenting great risks to mountain populations because of high transport competence and strong impact force (Blikra and Nemeč, 1998). In recent years, the number of wet avalanches has substantially increased due to warmer snow pack (Ancy and Bain, 2015). Their carrying capacity goes from smallest grains deposited by aeolian transport on the snow to large boulders (van Steijn et al., 1995; Blikra and Nemeč, 1998; Jomelli et al., 2007; Sæmundsson et al., 2008; Van Steijn, 2011). Typical avalanche debris zones were described, in French Alps crystalline rocks, to be composed of a source area consisting of steep rock walls, a transitional area and a terminal lobe. The latter is characterized by an elevation between 600 and 2400 m a.s.l., close to 0°C annual isotherm and slopes comprised between 15-27° (Jomelli et al., 2011). Avalanche deposit stratigraphy is close to debris flow deposits, the difference being that the snow matrix melts shortly after deposition, and was described by (Blikra and Nemeč 1998) as unsorted, scattered clasts and gravel patches infield with waterlain sand or pebbly sand. The avalanche processes in mountain terrains are generally controlled by both climate such as temperature and rainfall activity (van Steijn et al., 1995; Jomelli et al., 2011; Van Steijn, 2011) and local slope conditions (Blikra and Nemeč, 1998).

However, few remain known about the relationship between climate changes and avalanche recurrence over longer time periods. Reconstructing past avalanche dynamics in contexts of known climate changes could hence bring valuable new scientific data. Several studies exploring snow avalanche recurrence periods over the course of centuries to millennia in order to relate them to climate changes were led in particular in Norwegian lake sediment (Blikra and Nemeč, 1998; Seierstad et al., 2002; Nesje et al., 2007; Vasskog et al., 2011). These studies focused on the outlier presence of coarse particles in fine sediment. These coarse particles could have been incorporated into the sediment by different processes, such as i) transport by stream discharge of limited energy, which cannot explain the great number of such coarse grains; ii) lakeshore particles trapped in ice in the early winter then transported around the lake surface in the spring/early summer when the ice melts; or iii) snow avalanches eroding mineral-rich material and macroscopic plant remains on the slopes and transporting the debris to the frozen lake. To recover these coarse particles in the sediment cores, it is necessary to use a sieve to isolate, identify and count them, which is a destructive and time-consuming method. Several studies have explored snow avalanche



records in the Alps based on dendrochronological reconstructions (Casteller et al., 2007; Corona et al., 2010; Corona et al., 2013). All of them were limited by the age of the trees in the avalanche paths. In France, the risk related to
90 avalanches has been studied at a national scale since 1920 and has led to the “Enquête Permanente sur les
Avalanches” (EPA) database, which records the number of avalanches in specific paths. Studies exploring this record
through statistical analysis (Castebrunet et al., 2012; Eckert et al., 2013; Eckert et al., 2013b) have increased our
understanding of snow avalanches and their relationship with climatological conditions. However, this requires a
database composed of numerous records. There is thus a need to develop a new methodology to obtain continuous
95 reconstructions of past avalanches. In this study, we explored the potential of CT scanning to identify snow
avalanches record in lacustrine sediment. The main advantage of this technique is that it provides continuous and
non-destructive analysis.

Over the last 50 years, X-ray radiographs were initially used to explore the internal structure of sediment cores
(Bouma, 1964; Baker and Friedman, 1969) in order to optimize the opening process or even explore bioturbation
100 structures in the sediment (Howard, 1968). One of the technical problems was the loss of information with respect to
depth, as the radiographs are a plane representation of a 3D structure. In recent years, with improvements in X-ray
technology, CT scanning has been used to identify the sedimentary imprints of river floods (Støren et al., 2010) and
to explore sedimentary structures through 3D reconstructions (Pirlet et al., 2010; Bendle et al., 2015). A recent
review of CT scans in the geosciences (Cnudde and Boone, 2013) demonstrates the growing application possibilities
105 of this analysis as well as the limits of the technique. Furthermore, this review highlights the fact that this method has
never been used to reconstruct past snow avalanches.

The exploration of CT scan analysis as a new tool aims to develop a simpler, faster and non-destructive
methodology. We tested it in Lake Lauvitel located in the Oisans valley (western French Alps). This site has the
advantage of presenting steep slopes with three avalanche corridors ending directly in the lake. Some avalanches
110 have been observed in the spring, and snow accumulation is sometimes present at the base of the corridors. This site
is well suited to explore the reconstruction of an avalanche record based on avalanche deposits in a lacustrine
sedimentary sequence.

2 Materials and methods

1.1 Study site

115 Lake Lauvitel (44° 58' 11.4"N, 6° 03' 50.5" E) is located 1500 m above sea level (a.s.l.) in the Oisans valley of the
western French Alps, 35 km southeast of Grenoble. The lake covers an area of 0.35 km² and is 61 m deep, and the
total drainage area is approximately 15.1 km². The lake was created after a large rockslide dated to 4.7±0.4 10Be ka
(Delunel et al., 2010). The natural permeable dam created after this event caused a change in lake level of
approximately 20 m. Due to geomorphological settings, slopes around the lake are very steep and three avalanche
120 corridors (C1, C2, and C3) are present on the western side of the lake (Fig. 1b). They are accompanied by the
presence of snow accumulation at their bottom in spring (National Park ranger, Jérôme Forêt, pers. comm.), and
avalanches have been observed in C1 (Fig. 1e). The watershed bedrock consists mainly of granite and gneiss, with



125 minor outcrops of sedimentary rocks (Triassic limestone). The C1 track ends in an upper basin in the northern part of the lake, likely with no connection to the deeper part of the lake. C2 and C3 are located just above the coring location; there is no clear evidence of an obstacle preventing the sediment input from reaching the coring location. From the end of December to the beginning of May, the lake surface is frozen, and snow covers most of the watershed. The lake and its surroundings are situated in the Ecrins National Park restricted area.

Figure 1

130 1.2 Core description and methods

The core LAU11P2 (76 cm) was retrieved using a short UWITEC gravity corer to obtain a well-preserved interface, and LAU1104A (104.5 cm) was retrieved using a piston corer with a 90-mm sampling tube at the same location. The cores were split lengthwise and photographed at high resolution (20 pixels mm⁻¹). We examined in detail the visual macroscopic features of each core to define the different sedimentary facies to determine the stratigraphic correlation
135 between the two cores.

CT scanning was performed at Hopitiaux Universitaires de Genève (HUG) using a multidetector CT scanner (Discovery 750 HD, GE Healthcare, Milwaukee, Wis). The acquisition parameters were set as follows: 0.6-s gantry rotation time, 100 kVp, 0.984:1 beam pitch, 40-mm table feed per gantry rotation, and a z-axis tube current modulation with a noise index (NI) of 28 (min/max mA, 100/500) and a 64×0.625-mm detector configuration. All
140 CT acquisitions were reconstructed with the soft tissue and bone kernel. The images reconstructed with the bone kernel were used for subsequent analysis. The raw DICOM images were converted to an 8-bit .TIFF format using Weasis (v2.0.3) viewer. The radiograph resolution is 512×512 pixels, with up to 256 grey scale values. In this study, the sediment core was divided into 1,045 1-mm-thick frames, each pixel corresponding to a resolution of up to 500×500 μm and thus a voxel of 0.25 mm³. The images were then stacked using the Image J FIJI application, and
145 image treatments were performed using the 3D Object Counter plugin (Bolte and Cordelieres, 2006). First, we set a threshold to isolate the selected grey values, and we then applied a despeckle filter to remove the noise due to measurement. Finally 3D Object counter was used to reconstruct the particles and characterize them in a 3D coordinate system.

Grain size measurements were carried out on the core using a Malvern Mastersizer 800 particle-sizer at a lithology dependent sampling interval. Ultrasonics were used to dissociate particles and to avoid flocculation. Several layers of gravel-sized mineralogic particles were identified (Fig. 2) in the LAU1104 sediment core. To obtain a quantitative estimate of these particles, we passed samples through a 1-mm mesh and wet-sieved the sediment at variable intervals from 1 to 3 cm depending on the gravel concentration. The number of particles >2 mm and macro-remains present in the sieve were counted for each interval in the core LAU1104A.

155 The chronology of the Lake Lauvitel sediment sequence is based on short-lived radionuclide measurements. The short-lived radionuclides in the upper 75 cm of core LAU11P2 were measured using high-efficiency, very low-background, well-type Ge detectors at the Modane Underground Laboratory (LSM) (Reyss et al., 1995). The sampling intervals followed facies boundaries, resulting in a non-regular sampling of approximately 1 cm. Twelve



160 thick beds (at depths of 10.4-12.7, 17.3-19, 22.9-24.8, 29.7-30.9, 38-39, 40.6-42.4, 43.1-44.2, 45.7-50, 54.5-56.9, 60.4-62.5, 64.1-66 and 67.2-68.3 cm) were not analyzed because they were considered to be instantaneous deposits or part of an instantaneous deposit (see Results). ^{210}Pb excess was calculated as the difference between total ^{210}Pb and ^{226}Ra activities.

3 Results

3.1 Lithostratigraphy

165 The core lithology is composed of three facies. Facies 1 (F1) is silty-clay, dark-brown, finely laminated layer. It is interbedded by two other facies that are almost always associated with each other: Facies 2 (F2) is a normally graded bed from coarse sand to silt, sometimes with an erosive base; this facies is always associated with Facies 3 (F3), which is a thin white clay-rich layer. The presence of terrestrial macro-remains is sometimes identifiable in F2. A total of 18 normally graded beds are present in the core LAU1104A, with thicknesses ranging from 0.7 to 14 cm.
170 These are considered to be turbidites caused by heavy rainfall in the watershed (Støren et al., 2010; Giguët-Covex et al., 2012; Wilhelm et al., 2012a, 2012a, 2013; Gilli et al., 2013; Wilhelm et al., 2015). We did not observe a typical avalanche deposit facies in the split core. Sometimes, rare millimeter- to centimeter-scale grains are present in the turbidite deposits, but they are unlikely to have originated from the torrent due to the distance from the delta. The presence of gravel in the turbidites is interpreted to be the result of extreme rainfall triggering a flood and activating a debris flow in the avalanche corridor, transporting gravel from the steep slopes to the coring location.
175 analysis

The CT scan analysis is based on relative density. The histogram (Fig. 2a) represents the frequency of each of 1-255 levels of grey (0 is not shown on the graph due to overrepresentation corresponding to the background signal). Three modes representing the most frequent values are apparent in the histogram; they must be associated with certain types of sediment. The first mode is centered on the 106 value. After isolation, the corresponding elements in the sediment core were organic matter (OM) macroremains, such as a pinus twig found at 58 cm of depth (Fig. 2-E4). We thus selected the 95-125 range to identify OM. The second mode, centered on the 174 value, is relatively denser than OM. Its large spectrum and high count values correspond to the most common element in the sediment core, which would be the silty clay sedimentation matrix (Fig. 2b). The last mode is essentially the 255 level of grey.

185 Because it is the densest value possible, it corresponds to denser elements present in the silty-clay matrix. We selected the 240-255 value range and isolated them, and searched for corresponding particles in the sediment core. We identified gravel-sized granite elements in the sediment core (Fig. 2e1-2).

To compare objects counted numerically and objects counted manually, we need to know the size limit in units of volume (voxels), which is equivalent to 2-mm-diameter holes in a sieve. In 2D, a particle is retained in the sieve only if at least two sides are 2 mm in length, meaning at least two sides are 4 pixels long. Therefore, a particle of 16 (4x4) pixels with four sides that are 2 mm long will be retained in the sieve. However, if the same particle is missing 1 corner (minus three pixels, corresponding to a particle of 13 pixels), the particle would still be large enough to be retained in the sieve. This angular shape is more likely to be encountered in avalanche deposits; thus, we set the size



195 limit of the 3D Object Counter plugin to 13 pixels, which corresponds to 13 voxels. The organic macroremains are
composed of herbs, twigs or even roots, and their shapes were very complicated. Therefore, we did not choose any
volume limit in their identification process.

In the LAU1104A sediment core, a total of 499 gravel clasts equal to or larger than 13 voxels were identified. The
largest high-density object recovered from the core LAU1104A was an angular piece of granite of over 6 centimeter
on its longest side and weighing 206.03 g. Considering a density of 2.7, its volume can be estimated to be 76 307
200 mm³ ($\rho=m/V$). In comparison, the numerical volume is estimated to be 382,293 voxels, corresponding to 92,073
mm³. Thus, a difference of +17% in the volume for the CT counting is observed, probably due to pixel resolution.
The volume is thus overestimated, but still close to the actual rock volume.

We then compared the 3D Object Counter results and the coarse grains recovered from the sediment cores in slices
of variable thickness ranging from 1 to 3 cm. The depth 97-98 cm had no gravel > 2 mm in either the manual or
205 numerical counting (Fig. 2b, d). When considering a large amount of gravel, the manual and numerical counting
methods showed differences. For depths 15-18, 42-44, 44-46, 51-52, and 72-73 cm, the number of gravel clasts was
always underestimated by the numerical counting. As the 3D Object Counter plugin is identifying objects from one
pixel and its 8 neighbors in 2D and its 26 neighbors in 3D (Bolte and Cordelieres, 2006), the identification of objects
could vary, especially because of the noise treatment and when the object size is close to the image resolution. The
210 numerical counting result is slightly underestimated compared to the manual counting result (30% on average). The
depths 5-7 and 46-48 cm, on the contrary, showed an overestimation by the numerical counting (77% on average).
Considering the resolution, it is possible that a certain number of aggregated sand grains could have been considered
gravel by the numerical counting method, leading to an overestimation. This could be explained by the presence of
flood deposits in these two depths (Fig. 2d). Aggregated sand-sized elements would be considered by numerical
215 counting as larger elements, and the sand-sized elements are rounder and would go through the sieve, as opposed to
an angular particle of similar volume, which would be retained in the sieve. Overall, from this comparison between
the numerical and the manual counting and accounting for the previously mentioned CT scan bias, we obtained a
relatively well-constrained positive correlation ($r=0.79$, $n=8$; $p\text{-value}=0.0077$) (Fig. 2c).

The OM counting identified 7,413 objects, spread throughout almost every part of the sediment core. The largest OM
220 element found in the core was 6,949 voxels in size, corresponding to 1,732 mm³. This OM element was situated at a
depth of 58 cm in the middle of a flood deposit (Fig. 2d) and was identified as a pinus tree twig (Fig. 2e-4). In total,
89.2% of the numerically counted elements are under 3.25 mm³ (13 voxels), and almost every element recovered in
the sieve corresponded to small leaves, roots, twigs or herb macroremains (Fig. 2e-5).

Figure 2

225

3.3 Chronology

The ²¹⁰Pb excess profile (Fig. 3) showed a regular decrease punctuated by drops in ²¹⁰Pb_{ex} activities. Following
(Arnaud et al., 2002), these low values of ²¹⁰Pb_{ex} were excluded to construct a synthetic sedimentary record, because
these values are related to F2/F3 facies association, which is considered to be instantaneous turbidite deposits.



230 Plotting on a logarithmic scale, the $^{210}\text{Pb}_{\text{ex}}$ activities revealed a linear trend (Wilhelm et al., 2012b). Applying the
CFCS model (Goldberg, 1963), we obtain a mean accumulation rate of $3.7 \pm 0.3 \text{ mm yr}^{-1}$. The uncertainty in the
sedimentation rate was derived from the standard error of the CFCS model linear regression. Ages were then
calculated using the CFCS model applied to the original sediment sequence to provide a continuous age-depth
relationship. In addition, ^{137}Cs and ^{241}Am activity profiles present two peaks and one peak, respectively. The older
235 peak in ^{137}Cs activity at 28.1 cm is contemporary with the peak in ^{241}Am activity, allowing us to associate it to the
peak of nuclear weapons testing in the northern hemisphere in 1963. The younger peak in ^{137}Cs activity at 17.3 cm
can be attributed to fallout from the Chernobyl accident in 1986 (Appleby et al., 1991). These two artificial peaks are
in good agreement with the CFCS model (Fig. 3). In addition, we compared the historical flood calendar from the
Vénéon river valley to the instantaneous deposits recovered from the lake sediment for the last 100 years. In local
240 archives, seven major flood events occurred in 2008, 2003, 1987, 1962, 1955, 1922 and 1914, could be correlated to
the most important and recent graded deposits at depths of 0.4-2.9, 9.9-11.4, 18.7-20.1, 28.5-32.9, 38.2-39.6, 64.9-
66.7, and 67.7-69.1 cm, respectively. The good agreement between these independent chronological markers and the
 $^{210}\text{Pb}_{\text{ex}}$ ages strongly supports our age-depth model for the last century and validates our interpretation that the F2/F3
facies correspond to instantaneous flood deposits.

245 Figure 3

4 Discussion

We did not find any specific facies related to the avalanches deposits, as opposed to the floods deposits. The quantity
of sediment transported by a snow avalanche could be quite large and is characterized by very poor sorting and the
250 presence of organic matter (Blikra and Nemeč, 1998; Jomelli and Bertran, 2001). Snow avalanche materials can be
integrated into lacustrine sediments in two ways. In the case of a frozen lake, surface avalanche deposits are spread
across the ice and subsequently drop to the lake sediment from drifting ice. When an avalanche occurs while the lake
is ice-free, the avalanche deposits directly enter the water, and particles are concentrated in a more restricted area
closer to the avalanche corridor. As this is a very local phenomenon, the coring point has to be directly beneath the
255 avalanche corridor to record the maximum number of events, thus capturing both drop stones and direct avalanche
deposits. Lamination is present in the split sediment core despite of the presence of gravel-sized elements in the
sediment. We imagine that individual avalanches transported elements to the lake floor by gravity, but not enough
sediment is transported to create a specific facies. In the end, only the presence of coarse elements in the silty-clay
sediment matrix is characteristic of an avalanche deposit

260 Limits of counting: The numerical counting method using the CT scan radiographs is well suited for this type of
study because density differences between fine lacustrine sediments and coarse gravel is quite significant. The
centimeter-sized gravels found in sediment cores are also well suited to the resolution of the CT scan, especially
because the analysis of a volume as large as the more than one-meter-long sediment core allows for a pixel resolution
of only $500 \times 500 \mu\text{m}$. The good correspondence between the manual and numerical counting with respect to the



265 absence of gravel-sized element in the sediment should be highlighted. Additionally, the largest elements are well
identified, but smaller ones are more difficult to distinguish, as they are too close to the pixel resolution.
Discrepancies between the manual and numerical counting are hence quite important and probably related to the
image resolution. Thus, this study is limited to the presence of multiple gravel-sized elements in the sediment core.
The presence of more than one gravel-sized element along with organic macroremains is interpreted as a snow
270 avalanche deposit (Jomelli and Bertran, 2001; Nesje et al., 2007). In this context, the image resolution is precise
enough to identify coarse-grained layers but is not good enough to precisely characterize each grain, especially the
smallest ones. The CT scan is a powerful non-destructive tool for investigating the presence of coarse gravel-sized
elements inside lacustrine sediment cores and the presence of OM that could be a good way to identify precise depths
suitable for macroremain sampling for ^{14}C analysis.

275 The presence of gravel-sized rocks right in the middle of flood deposits enabled us to understand that the avalanche
corridors transport coarse sediment in more than one way. In this study, we consider a mountain watershed of a few
square kilometers. When a heavy rainstorm occurs, precipitation likely occurs throughout the whole watershed. The
main torrent would transport fine sediments into the lake and create a flood deposit. However, depending on the
rainfall intensity, smaller intermittent tributaries could also be activated, such as in the avalanches corridors,
280 triggering a debris flow and thus also transporting coarse grains to the lake bottom. This could explain the fact that
we found coarse grain sizes within several of the flood deposits in the sediment core. Debris flows are a different
phenomenon than wet avalanches, the former being mainly related to the precipitation regime (van Steijn, 1996) and
the latter being related to air temperature and snowpack structure (Ancy and Bain, 2015), which are, in the end, not
necessarily related to the climatological conditions. Consequently, to record only wet avalanches in the Lake
285 Lauvitel sediment sequence, we need to discriminate between gravel-sized sediment delivered to the lake by rainfall
or by avalanches. The presence of OM is less discriminant because it is found at almost all depths. Flood deposits,
considered to be instantaneous, are excluded from the age depth relationship. In this way, the coarse grains observed
in the resulting sediment core (without flood deposit) are only related to the wet avalanches of the specific corridors.

Figure 4

290 When applying the age model to the LAU1104A sediment core, we are able to express the number of rocks
identified since AD 1880 (Fig. 4) per 5-mm slice. We compared this with historic records of winters with higher
avalanche activity in the Oisans valley. The winter of 1922-1923 was an exceptional year in terms of winter
precipitation in the Oisans valley, and avalanches destroyed numerous buildings and covered roads with thick snow
deposits (Allix, 1923). The winter of 1969-1970 was also exceptional in terms of heavy snowfall, and no less than
295 800 avalanches were reported (Jail, 1970). On February 10th, 1970, an avalanche killed 39 people, making it the most
catastrophic avalanche in the last 200 years. In 1978, the Ecrins National Park rangers reported numerous avalanches
in the Oisans valley, especially in spring with wet snow avalanches temporarily blocking roads (Ecrins national park
internal report, 1978). The avalanche activity in the French Alps has also been explored based on the EPA since
300 1950. Four periods correspond to higher snow avalanche frequency in the northern French Alps: 1950-1955, 1968-
1970, 1978-1988, and 1993-1998 (Eckert et al., 2013) (Fig. 4). In the Lake Lauvitel sediment sequence, the periods
of increased numbers of rocks are 1888, 1898, 1920-1931, 1939, 1949, 1970-1972, 1977-1980 and 1990-1993. These



periods correspond roughly to higher avalanche activity in the previously mentioned records. They also correspond
to periods of four or more coarse particles present in the sediment core (5 mm slices) (Fig. 4). We thus set four rocks
305 as the minimum for recording wet avalanche deposits in Lake Lauvitel.

In Norway, similar avalanches in lake studies have been mostly related to winter precipitation (Seierstad et al., 2002;
Nesje et al., 2007; Vasskog et al., 2011), and this phenomenon was more frequent during cold periods, such as the
Younger Dryas or the Little Ice Age (Blikra and Nemeč, 1998). In the French Alps, the correlation between winter
precipitation and wet avalanche deposits seem probable, but due to the low quantity of information and the strong
310 interannual variability in precipitation, it is quite difficult to reach solid conclusions regarding this relationship. To
study this relationship, we need to develop long-term reconstructions of snow avalanche deposits, and the CT
scanning method allows us to do this for longer sediment archives.

One of the advantages of the CT scans and the 3D Object Counter (FIJI) is that each element identified as an object
is also characterized by x, y, z coordinates in the sediment core. We consider that a snow avalanche event is able to
315 transport many mineral elements of different sizes as well as OM; thus, this type of analysis opens new means to use
lake sediment to reconstruct past snow avalanche variability over long time periods.

5 Conclusion

CT scans are a well-developed analysis in the medical community and have been used for several geoscience-related
studies in the past decades. The principle of the analysis is based on differences in the relative densities of an object.
320 This study explores the possibility of using this technique on a lake sediment core to reconstruct a past snow
avalanche record. The analysis highlighted the presence of denser >2-mm mineralogical particles in the silty
sedimentary matrix, as well as the abundant organic matter, which could be a useful tool for sampling macroremains
for ¹⁴C analysis. Both of these features are typical of wet snow avalanche deposits, and a total of three avalanches
corridors are oriented directly into the western side of Lake Lauvitel. We interpreted the presence of both >2-mm
325 particles and organic matter deposited into the lake as a proxy for snow avalanche events. This methodology opens
new avenues for reconstructing past snow avalanche chronicles from lake sediment and for understanding avalanche
variability in regard to past and modern climate changes.

6 Acknowledgments

L. Fouinat's PhD fellowship was supported by a grant from Ecrins National Park, Communauté des Communes de
330 l'Oisans, Deux Alpes Loisirs and the Association Nationale de la Recherche et de la Technologie (ANRT). The
authors wish to thank Ecrins National Park for their authorization for sampling and assistance during the field work.
The authors thank the Laboratoire Souterrain de Modane (LSM) facilities for the gamma spectrometry measurements
and Hopitiaux Universitaires de Genève (HUG) for the CT scan analysis.



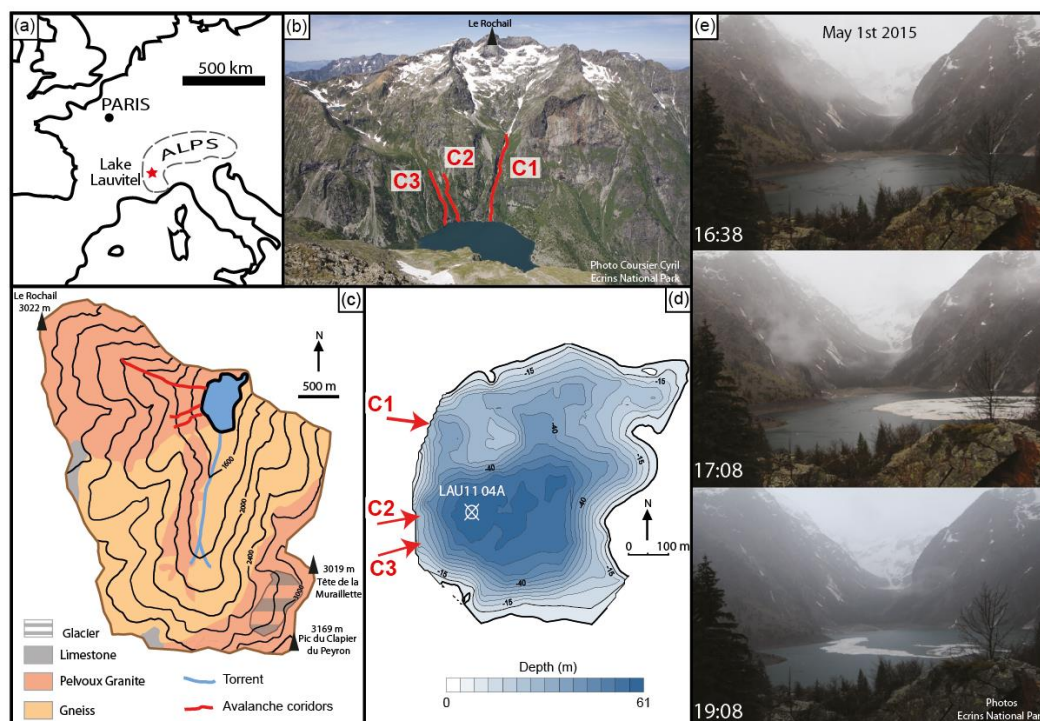
References

- 335 Allix, A., 1923. Les avalanches de l'hiver 1922-1923 en Dauphiné. *Rev. Géographie Alp.* 11, 513–527. doi:10.3406/rga.1923.5519
- Ancey, C., Bain, V., 2015. Dynamics of glide avalanches and snow gliding: GLIDE AVALANCHES AND SNOW GLIDING. *Rev. Geophys.* 53, 745–784. doi:10.1002/2015RG000491
- 340 Appleby, P.G., Richardson, N., Nolan, P.J., 1991. 241Am dating of lake sediments, in: Smith, J.P., Appleby, P.G., Battarbee, R.W., Dearing, J.A., Flower, R., Haworth, E.Y., Oldfield, F., O'Sullivan, P.E. (Eds.), *Environmental History and Palaeolimnology, Developments in Hydrobiology*. Springer Netherlands, pp. 35–42.
- Arnaud, F., Lignier, V., Revel, M., Desmet, M., Beck, C., Pourchet, M., Charlet, F., Trentesaux, A., Tribouvillard, N., 2002. Flood and earthquake disturbance of 210Pb geochronology (Lake Anterne, NW Alps). *Terra Nova*
- 345 14, 225–232.
- Baker, S.R., Friedman, G.M., 1969. A non-destructive core analysis technique using X-rays. *J. Sediment. Res.* 39, 1371–1383. doi:10.1306/74D71E2E-2B21-11D7-8648000102C1865D
- Bendle, J.M., Palmer, A.P., Carr, S.J., 2015. A comparison of micro-CT and thin section analysis of Lateglacial glaciolacustrine varves from Glen Roy, Scotland. *Quat. Sci. Rev.* 114, 61–77. doi:10.1016/j.quascirev.2015.02.008
- 350 Blikra, Nemeč, 1998. Postglacial colluvium in western Norway: depositional processes, facies and palaeoclimatic record. *Sedimentology* 45, 909–959. doi:10.1046/j.1365-3091.1998.00200.x
- Bolte, S., Cordelieres, F.P., 2006. A guided tour into subcellular colocalization analysis in light microscopy. *J. Microsc.* 224, 213–232.
- 355 Bouma, A.H., 1964. Notes on X-ray interpretation of marine sediments. *Mar. Geol.* 2, 278–309.
- Castebrunet, H., Eckert, N., Giraud, G., 2012. Snow and weather climatic control on snow avalanche occurrence fluctuations over 50 yr in the French Alps. *Clim. Past* 8, p–855.
- Casteller, A., Stöckli, V., Villalba, R., Mayer, A.C., 2007. An evaluation of dendroecological indicators of snow avalanches in the Swiss Alps. *Arct. Antarct. Alp. Res.* 39, 218–228.
- 360 Cnudde, V., Boone, M.N., 2013. High-resolution X-ray computed tomography in geosciences: A review of the current technology and applications. *Earth-Sci. Rev.* 123, 1–17. doi:10.1016/j.earscirev.2013.04.003
- Corona, C., Georges, R., Jérôme, L.S., Markus, S., Pascal, P., 2010. Spatio-temporal reconstruction of snow avalanche activity using tree rings: Pierres Jean Jeanne avalanche talus, Massif de l'Oisans, France. *CATENA* 83, 107–118. doi:10.1016/j.catena.2010.08.004
- 365 Corona, C., Saez, J.L., Stoffel, M., Rovera, G., Edouard, J.-L., Berger, F., 2013. Seven centuries of avalanche activity at Echalp (Queyras massif, southern French Alps) as inferred from tree rings. *The Holocene* 23, 292–304. doi:10.1177/0959683612460784
- Eckert, N., Keylock, C.J., Castebrunet, H., Lavigne, A., Naaim, M., 2013. Temporal trends in avalanche activity in the French Alps and subregions: from occurrences and runout altitudes to unsteady return periods. *J. Glaciol.* 59, 93–114. doi:10.3189/2013JoG12J091
- 370 Eckert, N., Lavigne, A., Castebrunet, H., Giraud, G., Naaim, M., 2013. Recent changes in avalanche activity in the French Alps and their links with climatic drivers: an overview, in: *International Snow Science Workshop (ISSW)*. Irstea, ANENA, Meteo France, p. p–1211.
- Giguet-Covex, C., Arnaud, F., Enters, D., Poulenard, J., Millet, L., Francus, P., David, F., Rey, P.-J., Wilhelm, B., Delannoy, J.-J., 2012. Frequency and intensity of high-altitude floods over the last 3.5ka in northwestern French Alps (Lake Anterne). *Quat. Res.* 77, 12–22. doi:10.1016/j.yqres.2011.11.003
- Gilli, A., Anselmetti, F.S., Glur, L., Wirth, S.B., 2013. Lake sediments as archives of recurrence rates and intensities of past flood events, in: *Dating Torrential Processes on Fans and Cones*. Springer, pp. 225–242.
- Goldberg, E.D., 1963. Geochronology with 210Pb. *Radioact. Dating* 121–131.
- 380 Howard, J.D., 1968. X-RAY RADIOGRAPHY FOR EXAMINATION OF BURROWING IN SEDIMENTS BY MARINE INVERTEBRATE ORGANISMS. *Sedimentology* 11, 249–258.
- Jail, M., 1970. Note sur l'hiver remarquable 1969-1970 dans les Alpes françaises. *Rev. Géographie Alp.* 58, 505–513. doi:10.3406/rga.1970.3495
- Jomelli, V., Bertran, P., 2001. Wet snow avalanche deposits in the French Alps: structure and sedimentology. *Geogr. Ann. Ser. Phys. Geogr.* 83, 15–28.
- 385 Jomelli, V., Brunstein, D., Grancher, D., Leone, F., Pavlova, I., Chenet, M., Utasse, M., 2011. Are Debris Floods and Debris Avalanches Responding Univocally to Recent Climatic Change-A Case Study in the French Alps. INTECH Open Access Publisher.



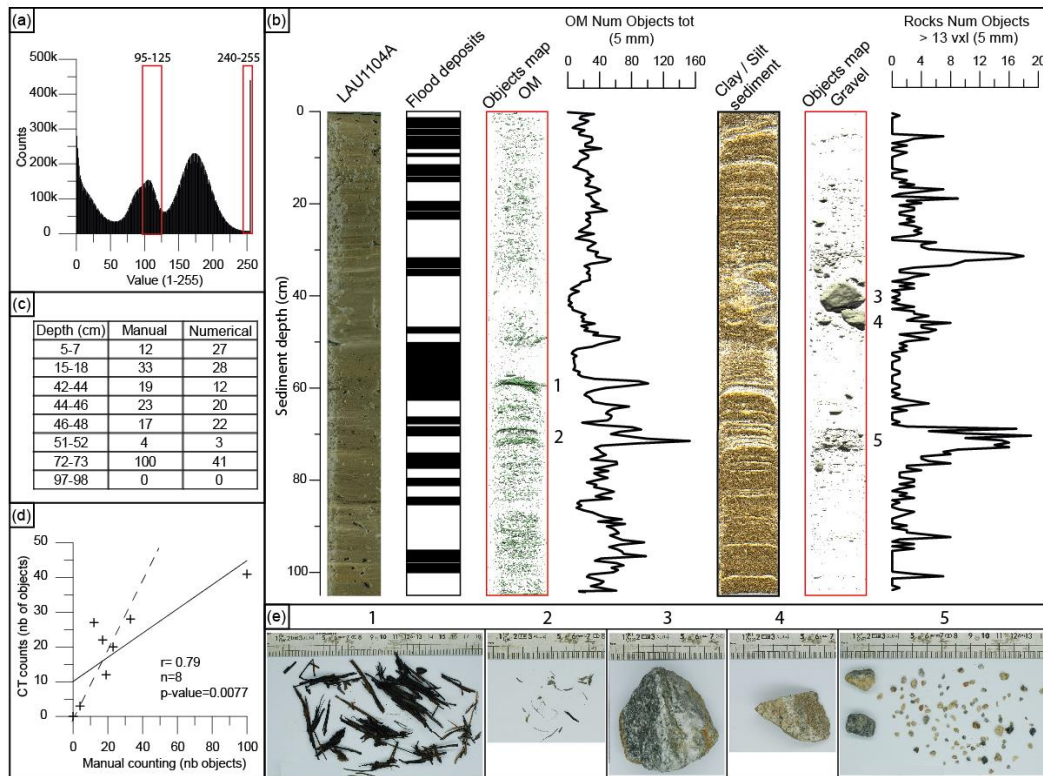
- 390 Jomelli, V., Delval, C., Grancher, D., Escande, S., Brunstein, D., Hetu, B., Filion, L., Pech, P., 2007. Probabilistic
 analysis of recent snow avalanche activity and weather in the French Alps. *Cold Reg. Sci. Technol.* 47,
 180–192.
- Nesje, A., Bakke, J., Dahl, S.O., Lie, O., Boe, A.-G., 2007. A continuous, high-resolution 8500-yr snow-avalanche
 record from western Norway. *The Holocene* 17, 269–277. doi:10.1177/0959683607075855
- 395 Pirlet, H., Wehrmann, L.M., Brunner, B., Frank, N., Dewanckele, J., Van Rooij, D., Foubert, A., Swennen, R.,
 Naudts, L., Boone, M., Cnudde, V., Henriet, J.-P., 2010. Diagenetic formation of gypsum and dolomite in a
 cold-water coral mound in the Porcupine Seabight, off Ireland: Diagenetic gypsum in a cold-water coral
 mound. *Sedimentology* 57, 786–805. doi:10.1111/j.1365-3091.2009.01119.x
- Reyss, J.-L., Schmidt, S., Legeleux, F., Bonté, P., 1995. Large, low background well-type detectors for
 measurements of environmental radioactivity. *Nucl. Instrum. Methods Phys. Res. Sect. Accel.*
 400 *Spectrometers Detect. Assoc. Equip.* 357, 391–397. doi:10.1016/0168-9002(95)00021-6
- Sæmundsson, P., Decaulne, A., Jónsson, H.P., 2008. Sediment transport associated with snow avalanche activity and
 its implication for natural hazard management in Iceland, in: *International Symposium on Mitigative
 Measures against Snow Avalanches*. pp. 137–142.
- 405 Seierstad, J., Nesje, A., Dahl, S.O., Simonsen, J.R., 2002. Holocene glacier fluctuations of Grovabreen and Holocene
 snow-avalanche activity reconstructed from lake sediments in Grningstlsvatnet, western Norway. *The
 Holocene* 12, 211–222. doi:10.1191/0959683602hl536rp
- Støren, E.N., Dahl, S.O., Nesje, A., Paasche, Ø., 2010. Identifying the sedimentary imprint of high-frequency
 Holocene river floods in lake sediments: development and application of a new method. *Quat. Sci. Rev.* 29,
 3021–3033. doi:10.1016/j.quascirev.2010.06.038
- 410 Van Steijn, H., 2011. Stratified slope deposits: periglacial and other processes involved. *Geol. Soc. Lond. Spec. Publ.*
 354, 213–226. doi:10.1144/SP354.14
- van Steijn, H., 1996. Debris-flow magnitude—frequency relationships for mountainous regions of Central and
 Northwest Europe. *Landslides Eur. Union* 15, 259–273. doi:10.1016/0169-555X(95)00074-F
- van Steijn, H., Bertran, P., Francou, B., Texier, J.-P., Héru, B., 1995. Models for the genetic and environmental
 415 interpretation of stratified slope deposits: Review. *Permafr. Periglac. Process.* 6, 125–146.
 doi:10.1002/ppp.3430060210
- Vasskog, K., Nesje, A., Storen, E.N., Waldmann, N., Chapron, E., Ariztegui, D., 2011. A Holocene record of snow-
 avalanche and flood activity reconstructed from a lacustrine sedimentary sequence in Oldevatnet, western
 Norway. *The Holocene* 21, 597–614. doi:10.1177/0959683610391316
- 420 Wilhelm, B., Arnaud, F., Sabatier, P., Crouzet, C., Brisset, E., Chaumillon, E., Disnar, J.-R., Guiter, F., Malet, E.,
 Reyss, J.-L., Tachikawa, K., Bard, E., Delannoy, J.-J., 2012a. 1400years of extreme precipitation patterns
 over the Mediterranean French Alps and possible forcing mechanisms. *Quat. Res.* 78, 1–12.
 doi:10.1016/j.yqres.2012.03.003
- 425 Wilhelm, B., Arnaud, F., Sabatier, P., Crouzet, C., Brisset, E., Chaumillon, E., Disnar, J.-R., Guiter, F., Malet, E.,
 Reyss, J.-L., Tachikawa, K., Bard, E., Delannoy, J.-J., 2012b. 1400years of extreme precipitation patterns
 over the Mediterranean French Alps and possible forcing mechanisms. *Quat. Res.* 78, 1–12.
 doi:10.1016/j.yqres.2012.03.003
- Wilhelm, B., Arnaud, F., Sabatier, P., Magand, O., Chapron, E., Courp, T., Tachikawa, K., Fanget, B., Malet, E.,
 430 Pignol, C., Bard, E., Delannoy, J.J., 2013. Palaeoflood activity and climate change over the last 1400 years
 recorded by lake sediments in the north-west European Alps. *J. Quat. Sci.* 28, 189–199.
 doi:10.1002/jqs.2609
- Wilhelm, B., Sabatier, P., Arnaud, F., 2015. Is a regional flood signal reproducible from lake sediments?
Sedimentology 62, 1103–1117. doi:10.1111/sed.12180

435



440

Figure 1: (a) Location of Lake Lauvitel, (b) Photo looking westward toward the location of the three avalanche corridors in the Lake Lauvitel watershed. (c) Simplified geologic map of the Lake Lauvitel watershed. (d) Lake Lauvitel bathymetric map and location of the three avalanche corridors and position of the LAU1104A coring point. (e) Photos of the lake looking to the south, with an avalanche entering the lake via the C1 corridor on May 1st 2015.



445 **Figure 2:** (a) Number of counts histogram for 1 to 255 levels of grey; selected range for OM (95-125) and for gravels (240-
 255) shown in red. (b) Selected depth for comparison between manual and numerical counts in core LAU1104A. (c)
 Correlation between manual and numerical rock counts, dashed line correspond to CT counts=Manual counts (d) From
 left to right: core LAU1104A photography, position of flood deposits, CT image stacks of both rocks and OM and
 450 corresponding totals summed at 5 mm intervals. (e) Photographs of organic matter (e1, e2) and gravel-sized elements (e3,
 e4, e5) recovered from the LAU1104 sediment core.

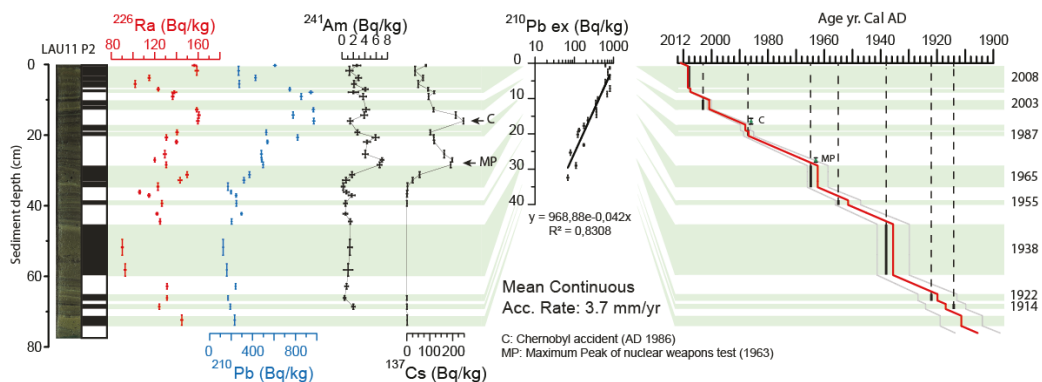
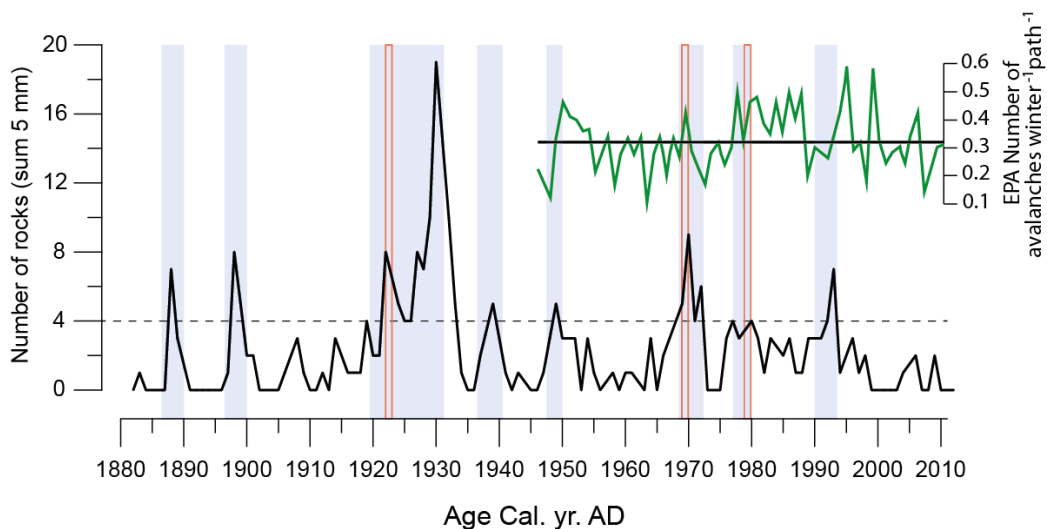


Figure 3: ^{226}Ra , ^{210}Pb , ^{241}Am , and ^{137}Cs activity profiles for core LAU11P2. Application of the CFCS model to the synthetic
 sedimentary profile of excess ^{210}Pb (without normally graded beds, which are considered to be instantaneous deposits).



455 **Resulting age-depth relationship with 1σ uncertainties and indications of historic flood dates associated with normally graded beds and the two artificial radionuclide markers.**



460 **Figure 4: Sum of rocks >13 voxels at 5 mm intervals identified in the LAU1104A sediment core since 1880 Cal. Yr. AD without the normally graded beds. The dashed line represents the threshold number from which avalanche periods are identified (highlighted in blue). Exceptional winters found in the bibliography are represented in red (Allix, 1923; Jail, 1970; Ecrins National Park internal report, 1978). EPA number of avalanches per path since AD 1950 in green, interannual mean value in black (N. Eckert et al., 2013).**

465

470

475

480

485